Supplement of

High-Elevation Meteorological Datasets from the Quelccaya Ice Cap and Surrounding Sites in the Cordillera Vilcanota, Peru

Perry et al.

S.1 Quality control procedures

Errors and gaps in meteorological observations are not uncommon, particularly in harsh, high-elevation sites where sensors are exposed to harsh environmental conditions, including strong winds, snowfall, icing, large temperature fluctuations, and intense solar radiation (Khadka et al. 2026). All available observations from the five AWSs were systematically inspected to identify erroneous or questionable measurements. The screening covered the complete period of record for each station and focused on temperature, relative humidity, incoming short-wave radiation, wind speed and direction, and snow depth. Because the measurement variables, length and continuity of the variables differ among stations, quality control was conducted separately for each station and variable.

Erroneous observations and unfiltered data can significantly compromise the interpretation of regional climatology. Anomalous values, including unrealistic measurements, abrupt discontinuities, and periods associated with known sensor malfunction, were identified from the individual time series. Records classified as erroneous were removed from the quality-controlled dataset and retained as missing values, for example we removed the wind speed data from Osjollo AWS site after the 21 January 2015 as the data found unrealistic (higher than usual and zero; check Metadata file).

Data gaps occurred at different times and for different variables across the five AWSs as a consequence of sensor malfunction, power or logging interruptions, complete or partial burial from snow, station maintenance, and the removal of observations during quality control. The periods and variables affected by these gaps are documented for each AWS are found in the corresponding metadata file, allowing users to assess data availability and identify periods for which individual variables should be used with caution.

Relative humidity measurements were corrected for subfreezing conditions because the sensor output was referenced to saturation vapour pressure over liquid water. For observations with air temperature below 0°C, the observed RH was corrected using WMO (2008), Alduchov and Eskridge (1996).

Particular attention was given to incoming shortwave radiation (SWin), which can be affected by sensor tilt and changes in the orientation of AWS structures, especially on snow- and ice-covered surfaces. Such problems can result in physically inconsistent measurements, particularly when measured outgoing shortwave radiation approaches or exceeds incoming shortwave radiation. Where required when albedo >0.95, SWin was therefore corrected following approaches previously applied to high-elevation AWS observations (Shea et al. 2015; Khadka et al. 2022). The correction uses the relationship between measured incoming and outgoing shortwave radiation and an assumed physically plausible maximum surface albedo to reconstruct affected SWin values.

- Equation albedo = SWout/SWin

Unrealistic wind speed values were removed, for example sudden change in the pattern for the whole period which might be because of the malfunction of the sensors. Records for both wind speed and wind direction were zero were also excluded, assumed as the ice riming stopped the sensor.

Depending on the precipitation-gauge shielding configuration, separate wind-induced undercatch correction functions were applied for the single-shielded Lake Sibinacocha and the Belfort double-shielded Quelccaya Pluvio^2 weighing precipitation gauges. For Lake Sibinacocha, liquid precipitation was corrected using the relationships of Masuda et al. (2019), whereas mixed and solid precipitation were corrected using phase-specific transfer functions from Kochendorfer et al. (2017). For Quelccaya, mixed and solid precipitation were corrected following Kochendorfer et al. (2018), while liquid precipitation was retained unchanged because no corresponding correction function was implemented. For unshielded and single-shielded gauges, wind speed was limited to 7.2 m s^{-1} when applying the mixed- and solid-phase transfer functions, whereas a maximum wind speed of 6.1 m s^{-1} was used for double-shielded gauges. The precipitation phase was classified as liquid at air temperatures >2°C, mixed between 0 and 2°C, and solid below 0°C. More robust methods to quantify the relative percentages of LE Precipitation phase using co-located Parsivel observations are outlined in Graves et al. (2026) but were beyond the scope of this paper.

S2. Relative Humidity correction

A column with the corrected relative humidity is also added with the measured data. Relative humidity measurements were assumed to be referenced to saturation vapour pressure over liquid water (RH). Under subfreezing conditions, RH was converted to relative humidity with respect to ice (RHi) using temperature-dependent saturation vapour pressures over water and ice.

Saturation vapour pressures over water and ice were calculated using Magnus-type formulations recommended for meteorological applications (WMO, 2008; Alduchov and Eskridge, 1996):

$$e_{sw} = 6.112 \times \exp\left(\frac{17.625 \times T}{243.04 + T}\right)$$

$$e_{si} = 6.112 \times \exp\left(\frac{22..46 \times T}{272.62 + T}\right)$$

where T is air temperature in °C and saturation vapour pressure is expressed in hPa. was subsequently calculated as

$$RH_i = \text{RH} \times \frac{e_{sw}}{e_{si}}$$

S3. Actual vapour pressure

Then the actual vapour pressure (hPa) is calculated from and relative humidity (RHi), which ranges from 0 to 100%:

$$e_a = e_{s(i/w)} \times RH_i$$

S4. Relative humidity and saturation vapor pressure

Relative humidity exhibited an equally pronounced seasonal cycle. Relative humidity with respect to water (RHw) reached its highest seasonal values during DJF at all four stations, ranging from 79% at Murmurani Alto to 93% at Quelccaya. RHw decreased substantially toward JJA, reaching 54% at Murmurani Alto, 67% at Quelccaya, and 55% at Sibinacocha Dam. Three-year hydrological-year mean RHw was 68% at Murmurani Alto, 82% at Quelccaya, and 69% at Sibinacocha Dam. Osjollo Anante and Quelccaya consistently recorded higher relative humidity than Murmurani Alto and Lake Sibinacocha during the seasons for which observations were sufficiently complete (Table S1), consistent with their higher elevation and colder conditions.

Saturation vapor pressure followed the seasonal temperature cycle, whereas actual vapour pressure reflected variations in both air temperature and relative humidity. At the lower elevation stations, higher temperatures resulted in greater saturation and actual vapour pressures despite generally lower relative humidity. Hydrological-year mean actual vapour pressure was 4.4 hPa at Murmurani Alto, 3.6 hPa at Quelccaya, and 4.8 hPa at Lake Sibinacocha.

S5. Lake Sibinacocha Pluvio^2 vs. Tipping Bucket Comparison

At Lake Sibinacocha, hydrological year precipitation measured by the Pluvio^2 and tipping-bucket gauges showed generally close agreement, although differences varied among years (Fig. S11; Table S5). Annual totals ranged from 582 (2022-23) to 967 mm (2021-22) for the Pluvio^2 and from 579 to 940 mm for the tipping bucket. Differences between the two gauges ranged from −80 to +68 mm, with almost identical totals in 2018–2019 and 2022–2023. Across the full 2017–2018 to 2024–2025 period, the Pluvio^2 recorded slightly less precipitation overall than the tipping bucket, but the relatively small inter-gauge differences indicate broadly consistent interannual variability at the site. Analysis of the daily timing of precipitation indicated much larger discrepancies between the Pluvio^2 and the tipping bucket gauge (Fig. S12). Both the Pluvio^2 and Parsivel data confirm the late afternoon convective and overnight stratiform precipitation largely falls as snow, but this snow was not recorded as liquid equivalent precipitation in the unheated tipping bucket until the next morning when it began to melt in full sun.

Table S1. Seasonal (SON = September, October, and November; DJF = December, January, and February; MAM = March, April, and May; JJA = June, July, and August) and annual (September to August -- hydrological year) mean values of selected meteorological variables measured at four automatic weather stations (AWSs). Statistics are presented for September 2012–August 2015 at Murmurani Alto and Osjollo Anante, and for September 2018–August 2021 at Quelccaya and Sibinacocha Dam. Seasonal or annual mean values are discarded when data gaps exceed 10% of the data period.

Variables	Stations	SON	DJF	MAM	JJA	Hydrological year mean
RHw (%)	Murmurani Alto	66.9	79.3	71.3	53.7	67.7
RHw (%)	Osjollo Anante	76.0	88.1	79.6		
RHw (%)	Quelccaya	82.8	92.8	86.1	67.2	82.2
RHw (%)	Sibinacocha	69.2	80.6	72.2	54.5	69.1
e_a(hPa)	Murmurani Alto	4.4	5.5	4.8	3.1	4.4
e_a(hPa)	Osjollo Anante	3.8	4.5	3.9		
e_a(hPa)	Quelccaya	3.7	4.5	3.9	2.5	3.6
e_a(hPa)	Sibinacocha	4.8	5.9	5.2	3.2	4.8
Corrected PRECIP (mm)	Quelccaya	311	555	301	47	1214
Corrected PRECIP (mm)	Sibinacocha	201	446			

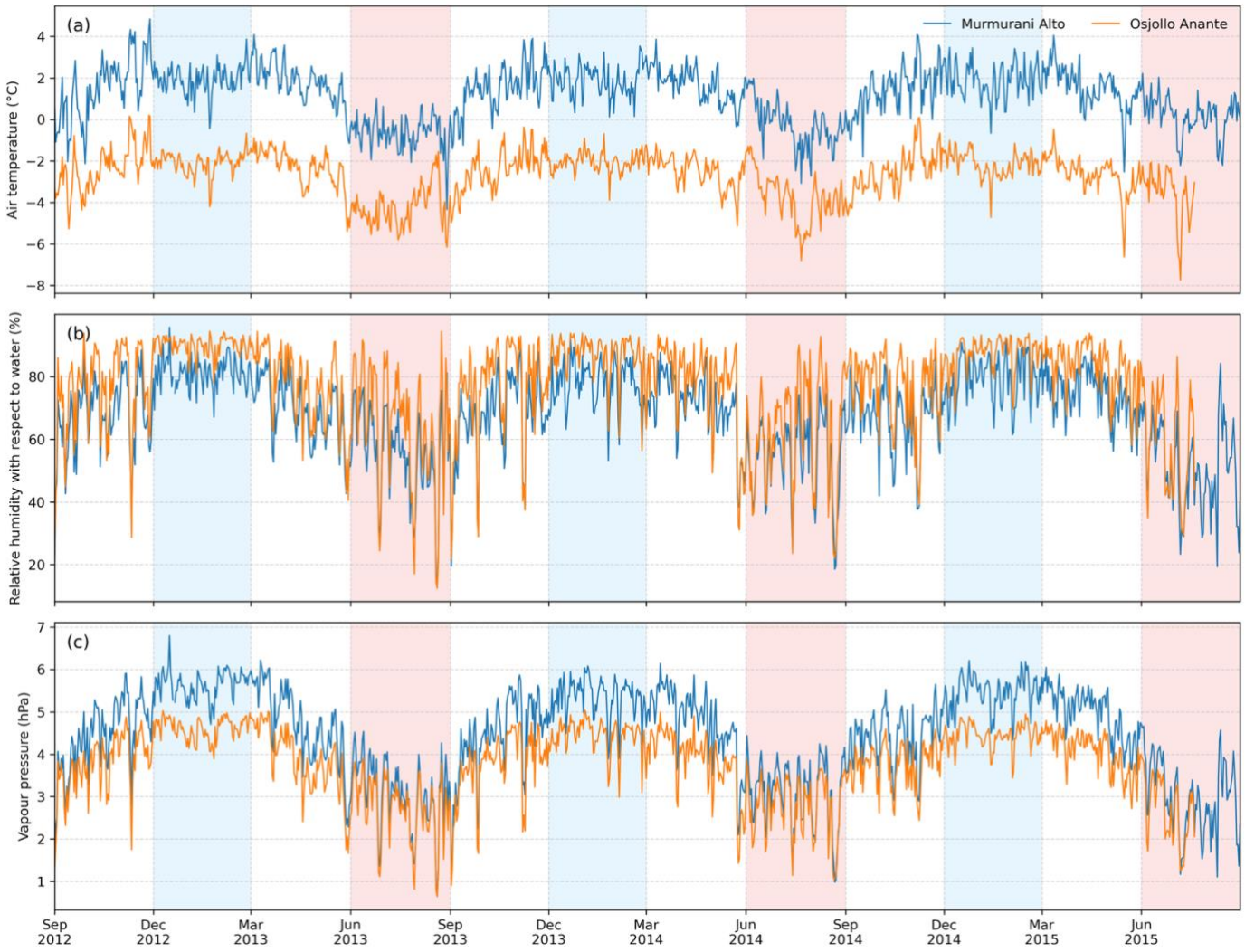


Figure S1. Mean daily air temperature, relative humidity and vapor pressure between the Murmurani and Osjollo Anante AWSs for the period between September 2012 to August 2015. The shaded background denotes the different seasons (SON = September, October, and November; DJF = December, January, and February; MAM = March, April, and May; JJA = June, July, and August).

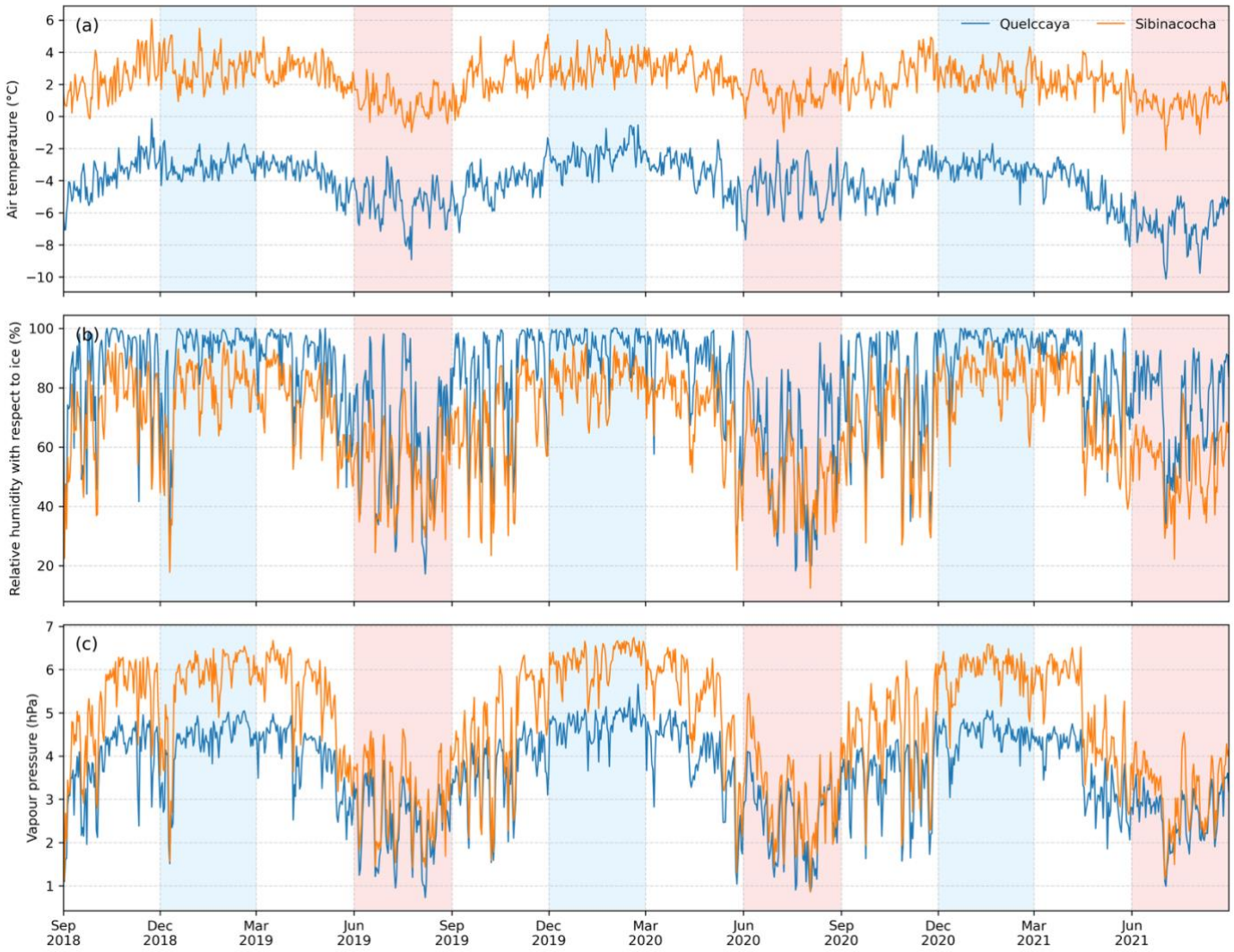


Figure S2. Mean daily air temperature, relative humidity and vapor pressure between the Quelccaya and Sabinacocha AWSs for the period between September 2018 to August 2021. The shaded background denotes the different seasons (SON = September, October, and November; DJF = December, January, and February; MAM = March, April, and May; JJA = June, July, and August).

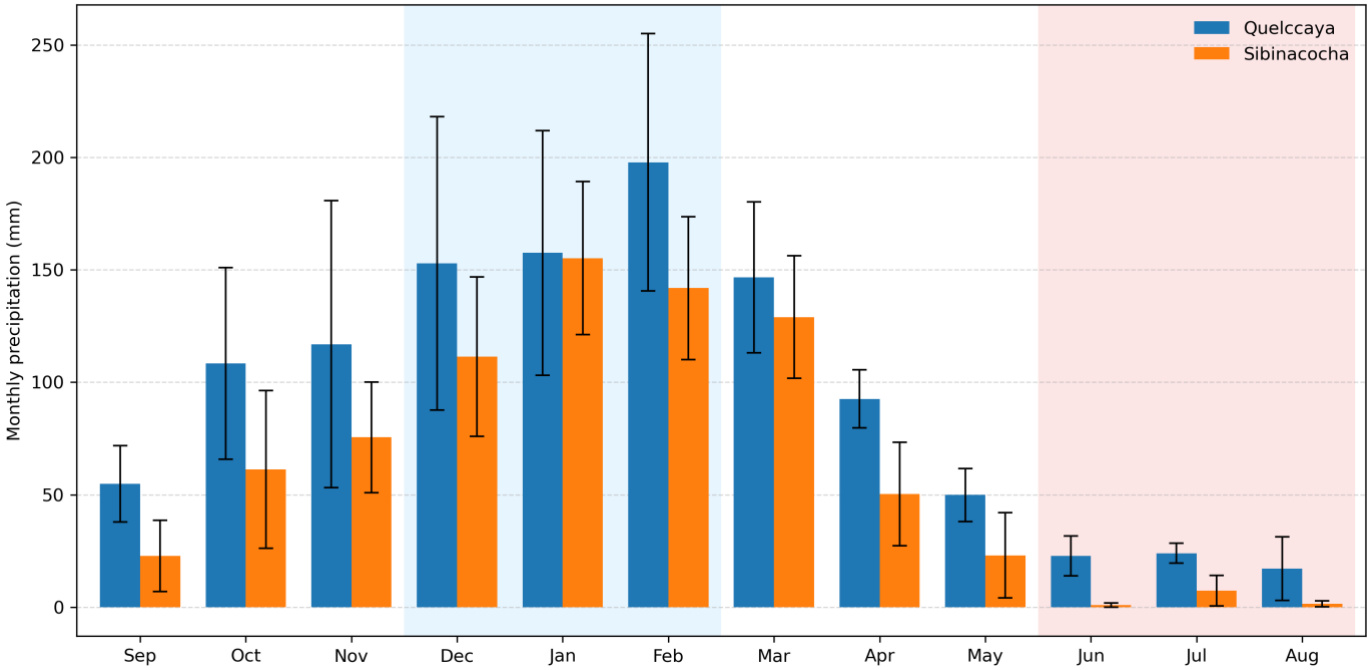


Figure S3. Mean monthly precipitation (uncorrected) at Quelccaya and Sibinacocha AWSs between September 2018-August. The shaded background denotes the different seasons (SON = September, October, and November; DJF = December, January, and February; MAM = March, April, and May; JJA = June, July, and August) 2021.

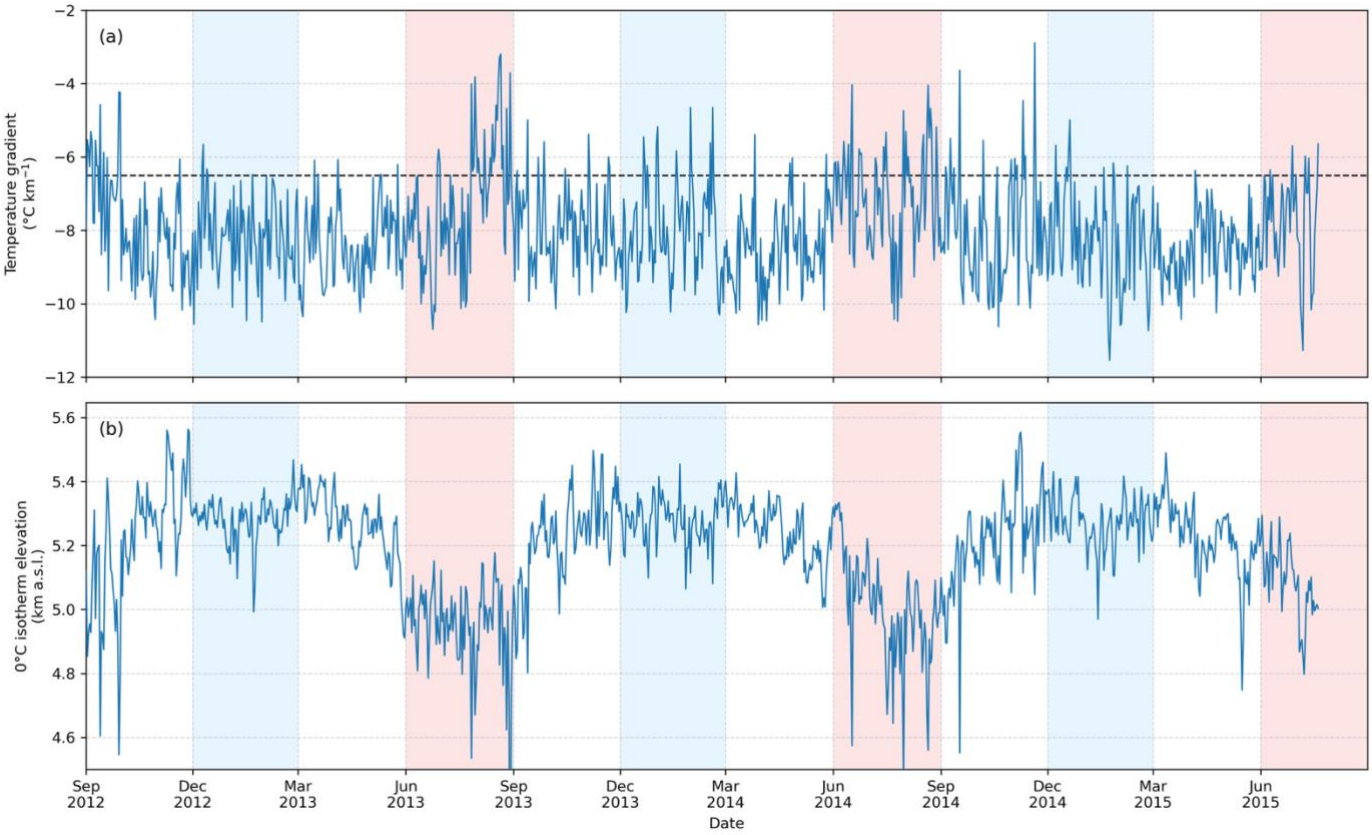


Figure S4: Mean daily temperature gradient (top) and 0°-isotherm elevation (bottom) between the Murmurani and Osjollo AWSs. The shaded background denotes the different seasons (SON = September, October, and November; DJF = December,

January, and February; MAM = March, April, and May; JJA = June, July, and August

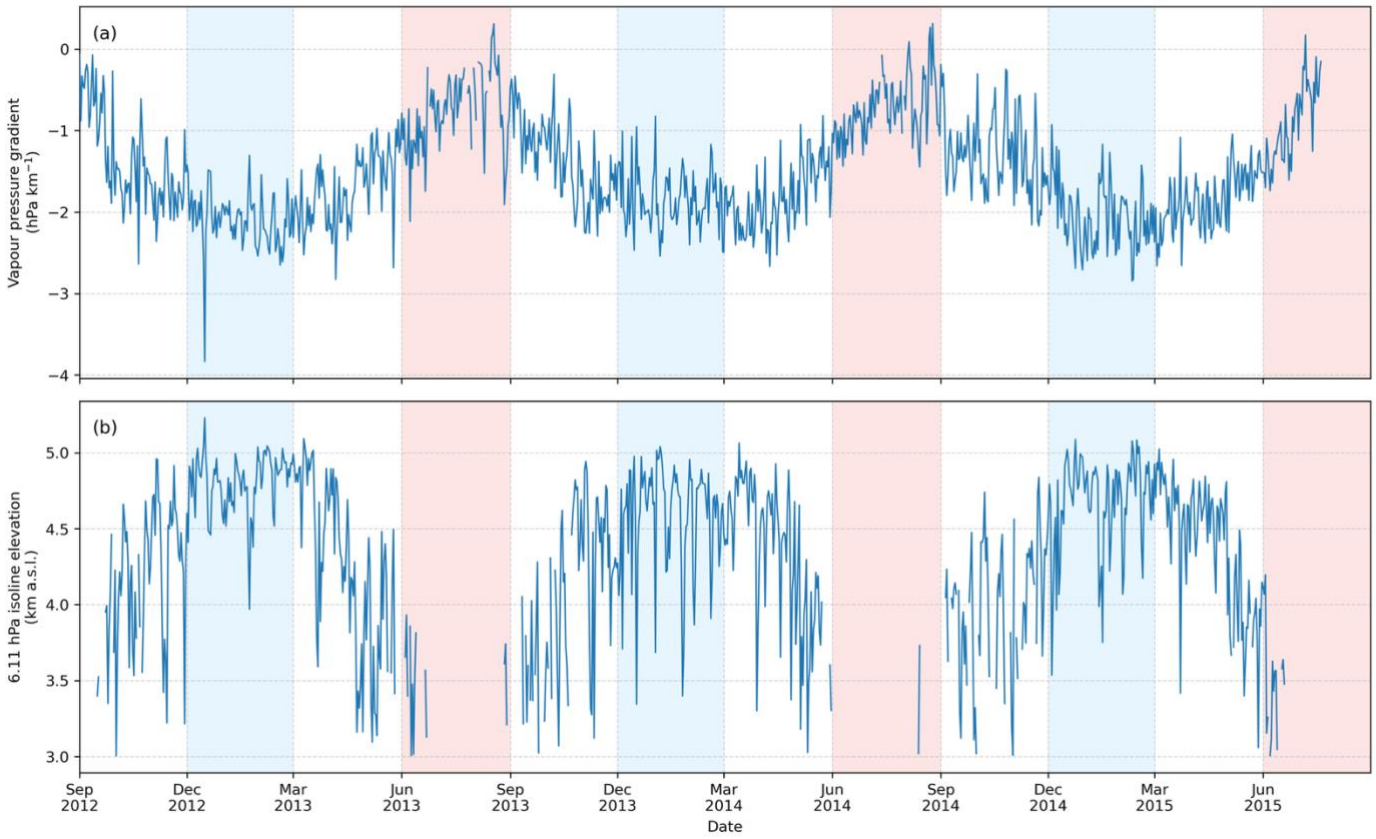


Figure S5: Mean daily vapour pressure gradient and 6.11 hPa isoline between the Murmurani and Osjollo AWSs. The shaded background denotes the different seasons (SON = September, October, and November; DJF = December, January, and February; MAM = March, April, and May; JJA = June, July, and August).

Table S2. Mean seasonal air temperature lapse rate (LR), zero-degree (0°)isotherm elevation, vapour pressure gradient (VPG) and 6.11 hPa isoline elevation ( ) for different season calculated from the in situ data from Murmurani and Osjollo AWSs for September 2012 to August 2015.

Seasons	LR (°C km^{-1})	0° isotherm (km)	VPG (hPa km^{-1})	Ze_a= 6.11 (km)
SON	-8.0 ± 1.3	5.219 ± 0.16	-1.4 ± 0.6	
DJF	-8.2 ± 1.2	5.277 ± 0.073	-2.0 ± 0.4	4.687 ± 0.289
MAM	-8.5 ± 1.0	5.224 ± 0.102	-1.8 ± 0.4	4.326 ± 0.493
JJA	-7.3 ± 1.5	4.975 ± 0.167	-0.7 ± 0.4	

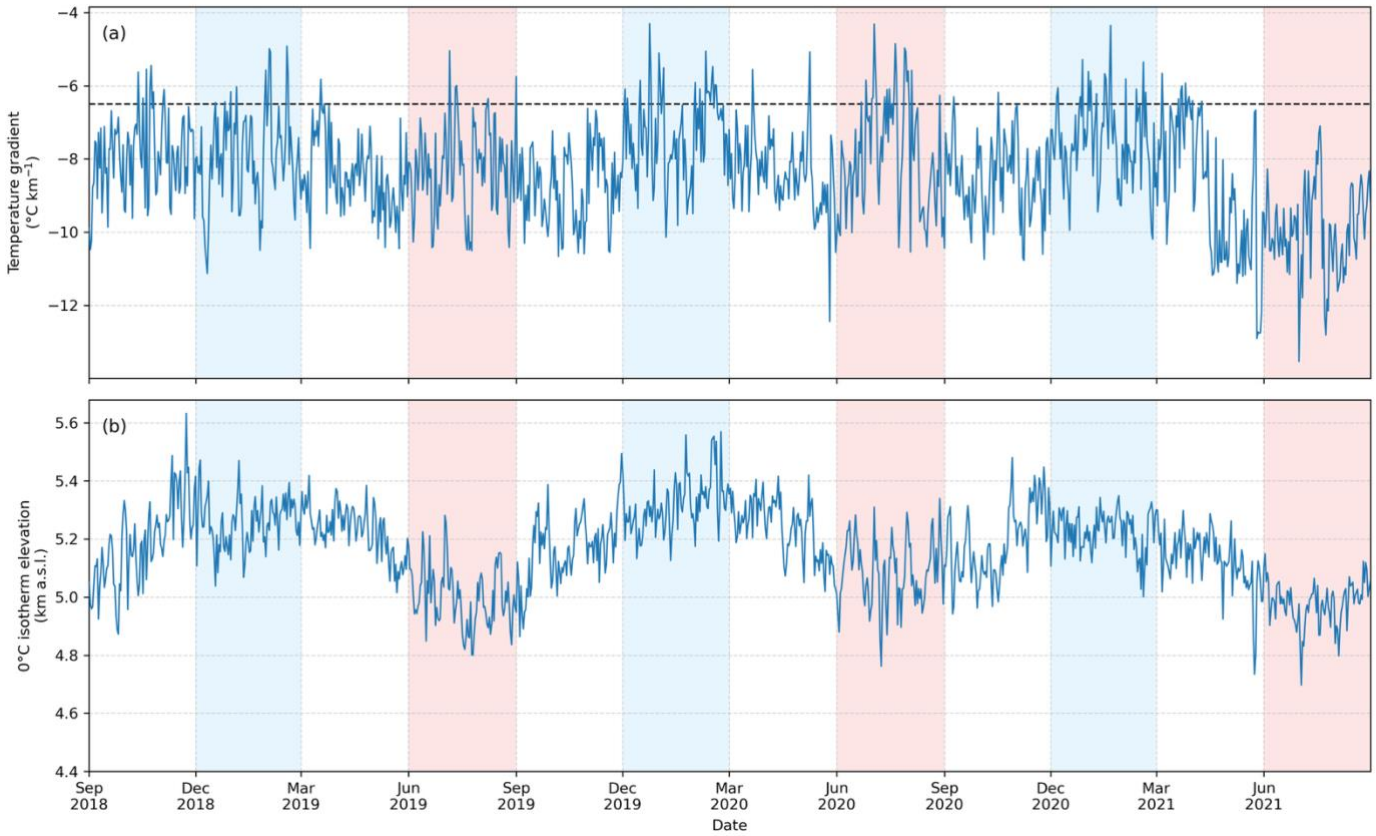


Figure S6. Mean daily temperature gradient (top) and 0-degree isotherm elevation (bottom) between the Quelccaya and Sibinacocha AWSs. The shaded background denotes the different seasons (SON = September, October, and November; DJF = December, January, and February; MAM = March, April, and May; JJA = June, July, and August)

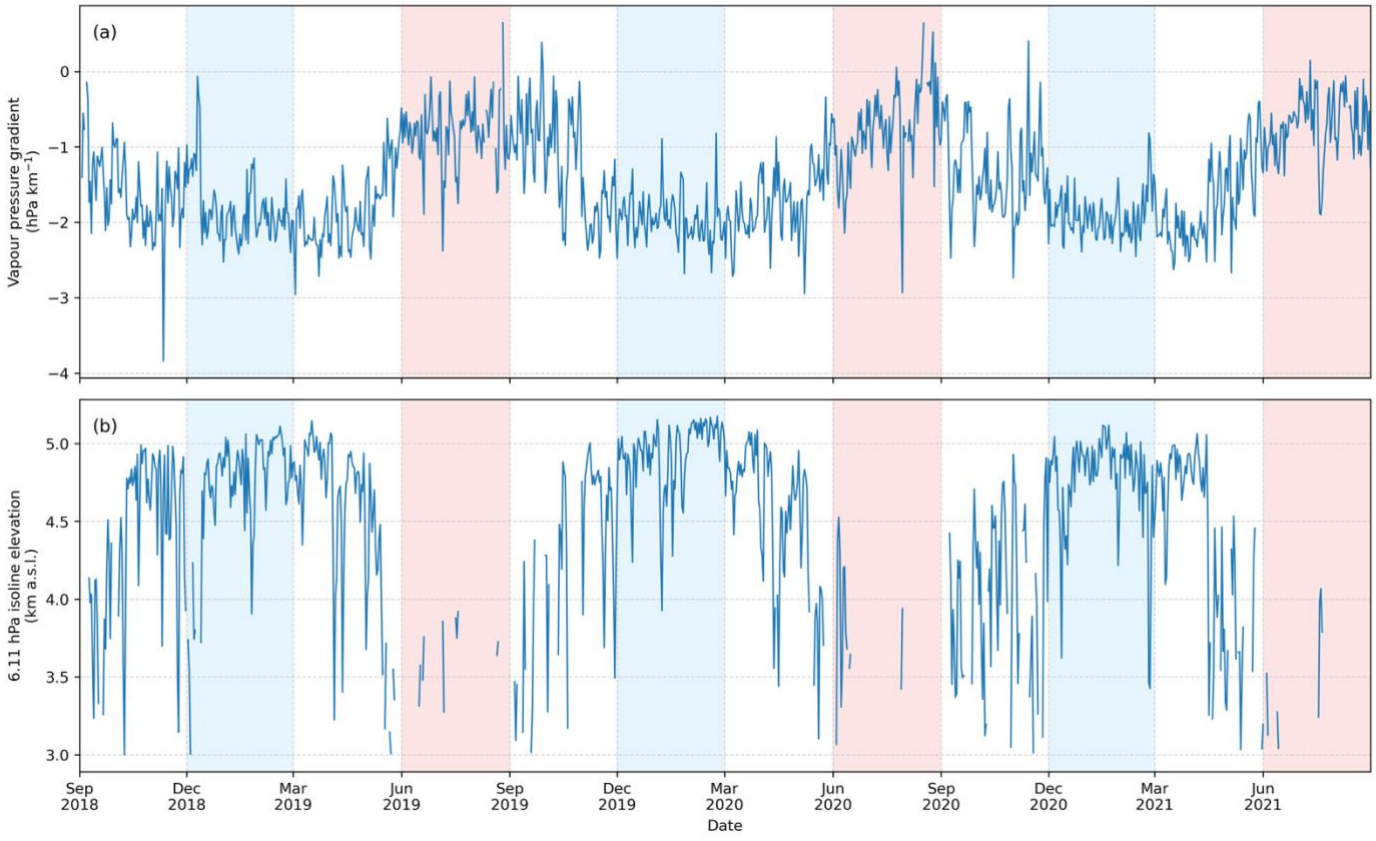


Figure S7. Mean daily vapour pressure gradient and 6.11 hPa isoline between the Quelccaya and Sibinacocha AWSs. The shaded background denotes the different seasons (SON = September, October, and November; DJF = December, January, and February; MAM = March, April, and May; JJA = June, July, and August)

*Table S3. Mean seasonal air temperature lapse rate (LR), zero-degree (0°) isotherm elevation, vapour pressure gradient (VPG), 6.11 hPa isoline altitude (*Zea=6.11*) for different season calculated from the in situ data from Sibinacocha and Quelccaya AWSs*

Season	LR (°C km^{-1})	0° isotherm (km)	VPG (hPa km^{-1})	Ze_a=6.11 (km)
SON	-8.2 ± 10	5.177 ± 0.129	-1.6 ± 0.6	
DJF	-7.6 ± 1.2	5.27 ± 0.088	-1.9 ± 0.4	4.805 ± 0.294
MAM	-8.4 ± 1.1	5.213 ± 0.100	-1.8 ± 0.5	4.540 ±0.539
JJA	-8.5 ± 1.3	4.993 ± 0.105	-0.9 ± 0.5	

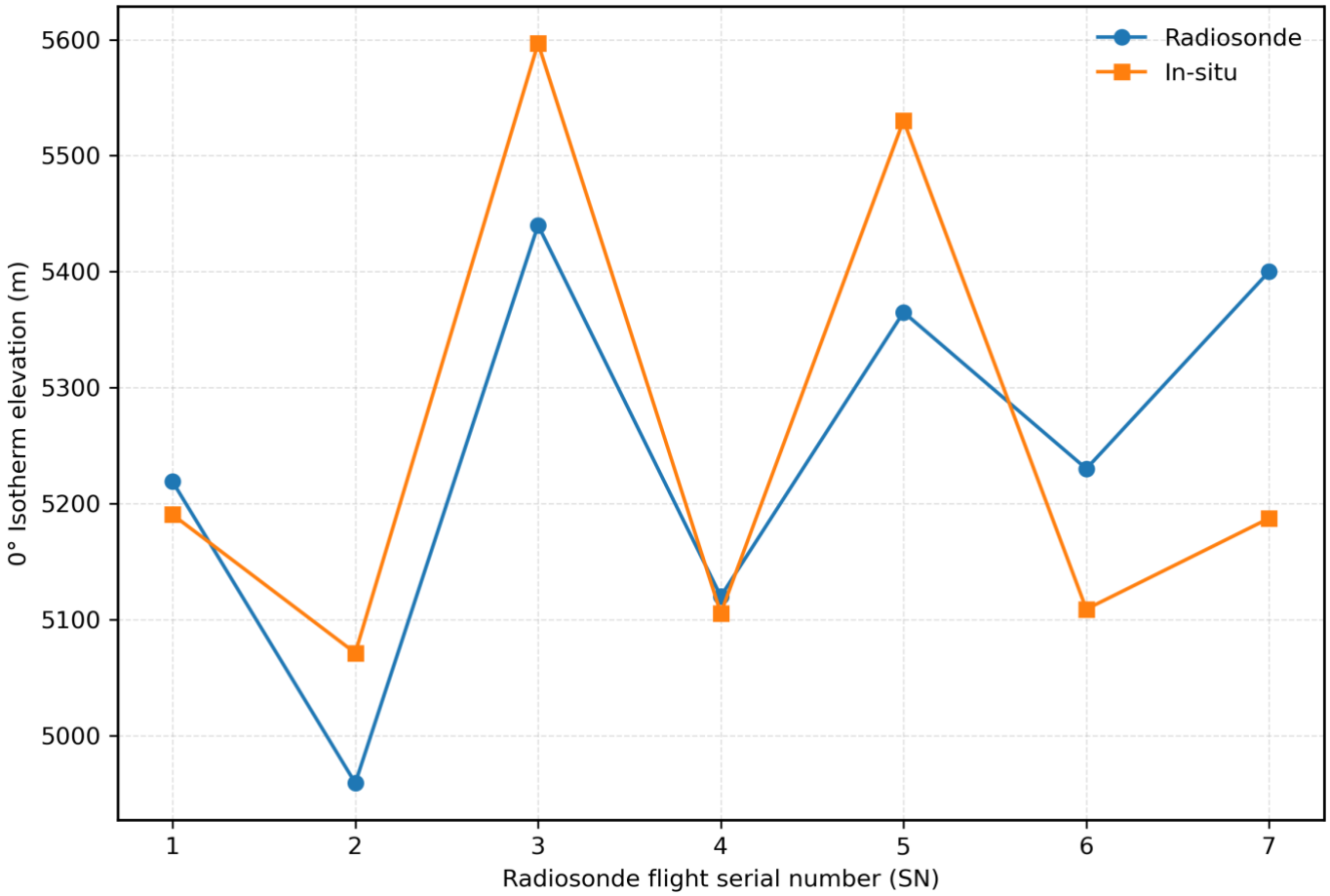


Figure S8. Comparison of the 0° isotherm elevation from the radiosonde and the calculated 0° isotherm elevation from the Sibinacocha and Quelccaya AWSs data.

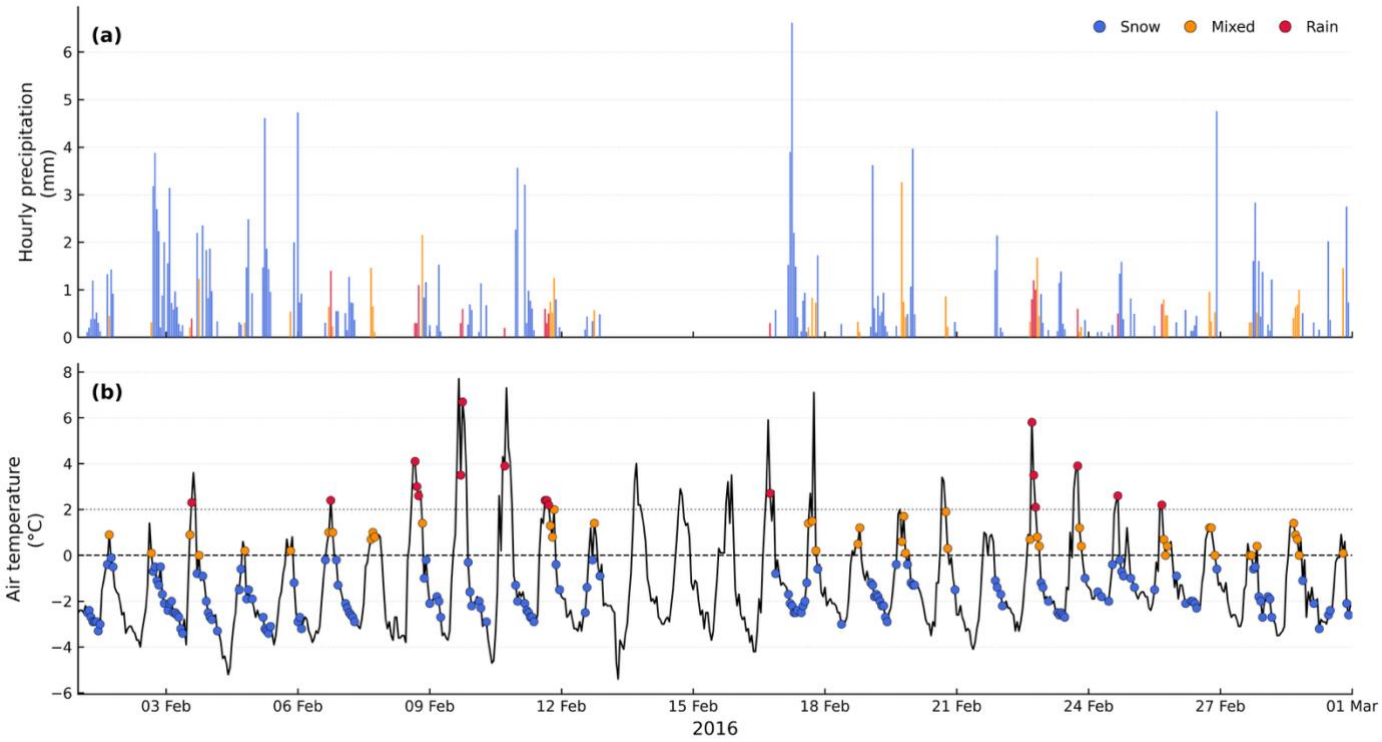


Figure S9. (a) Hourly precipitation rates (snow, mixed, and rain) during February 2016, and (b) corresponding hourly temperatures annotated with observed precipitation types (snow, rain, or mixed).

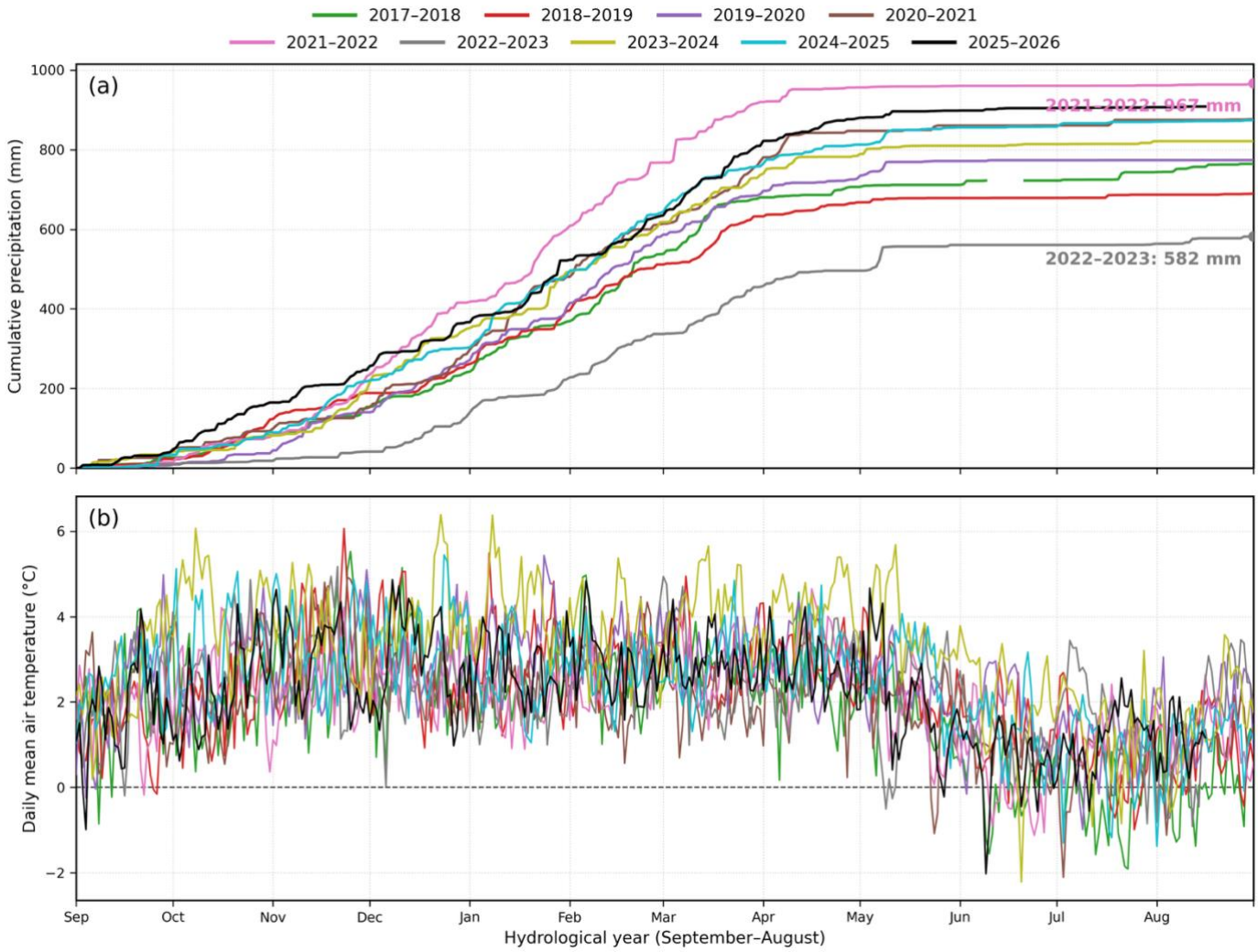


Figure S10. Cumulative precipitation and mean daily air temperature at Sibinacocha AWS for different hydrological years.

Table S4. Date, location and 0° isotherm elevation from the radiosonde and the calculated 0° isotherm elevation from the Sabinacocha and Quelccaya AWSs data.

SN	Date	Latitude (°)	Longitude (°)	Radiosonde started Elevation (m)	0° Isotherm radiosonde (m)	0° isotherm calculated from the AWS data (m)	Bias (m)
1	2018030400	-13.8819	-71.2245	4329	5219	5190	29
2	2018030406	-13.8818	-71.2245	4329	4959	5071	-112
3	2018030418	-13.8955	-70.9744	4720	5440	5597	-157
4	2018030501	-13.8955	-70.9744	4720	5120	5105	15
5	2018030519	-13.8955	-70.9744	4720	5365	5530	-165
6	2018030600	-13.8955	-70.9744	4720	5230	5109	121
7	2018030700	-13.8955	-70.9744	4720	5400	5187	213
8	2018030818	-13.3116	-71.5753	3365	5210	5449	-239

9	2018030900	-13.3116	-71.5753	3365	5290	4920	370
10	2018031000	-13.5205	-71.96008	3365	5095	5064	31
11	2018031018	-13.5205	-71.96008	3365	5350	5579	-229

Table S5. The total hydrological year precipitation from Pluvio² and tipping bucket at Lake Sibinacocha.

Hydrological year	Pluvio² (mm)	Tipping bucket (mm)	Difference (Pluvio² – Tipping bucket in mm)
2017-2018	764	845	-80
2018-2019	690	690	0
2019-2020	774	820	-46
2020-2021	876	808	68
2021-2022	967	925	42
2022-2023	582	579	3
2023-2024	822	851	-30
2024-2025	874	940	-66
2025-2026	909	965	-

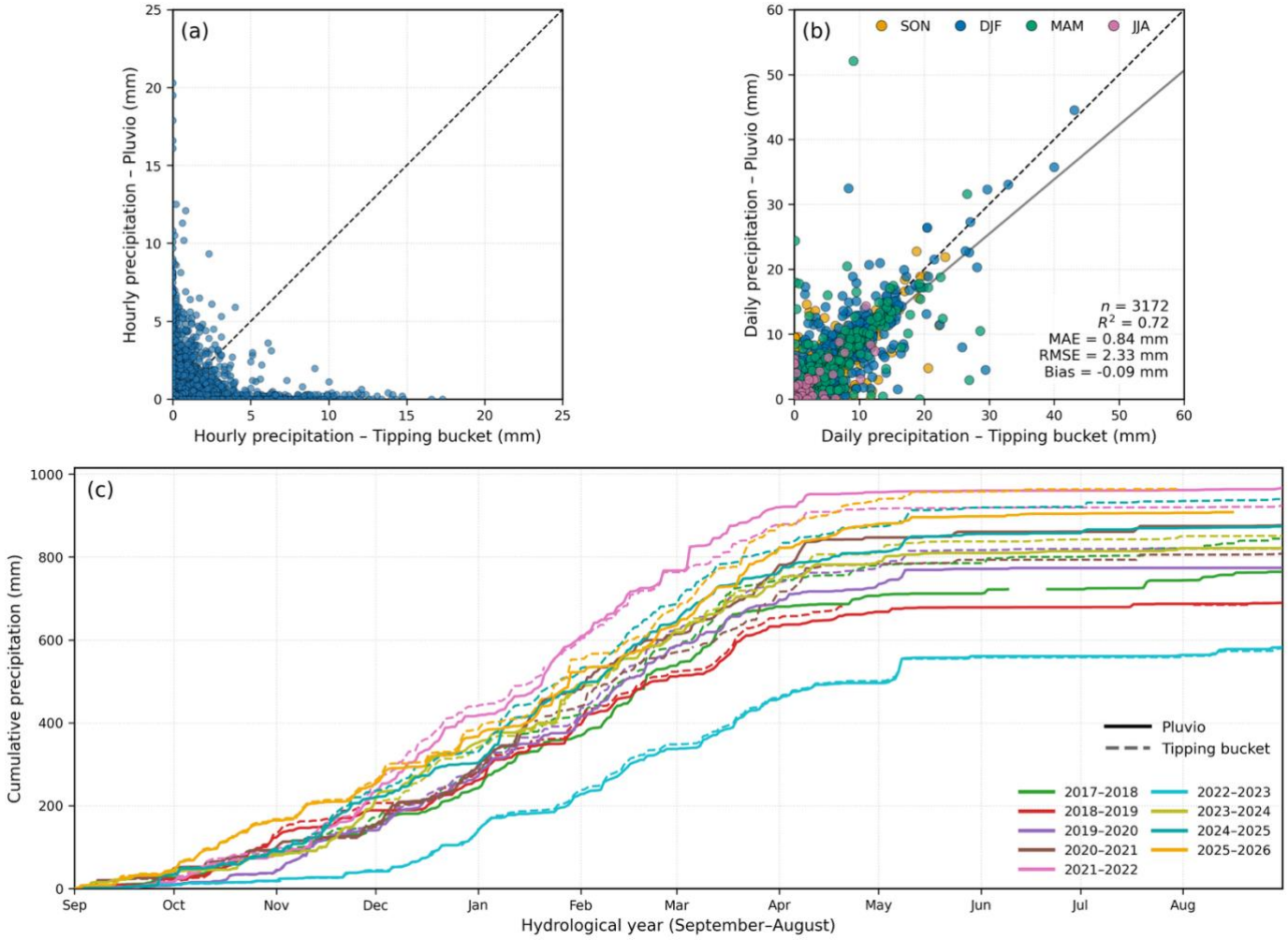


Figure S11. Precipitation comparison measured from the Pluvio² and Tipping bucket at Sibinacocha AWS site. a) Hourly

precipitation b) daily precipitation and different colour is for different seasons and overall metrics of comparison and c) cumulative precipitation for different hydrological years from the Pluvio² and Tipping bucket.

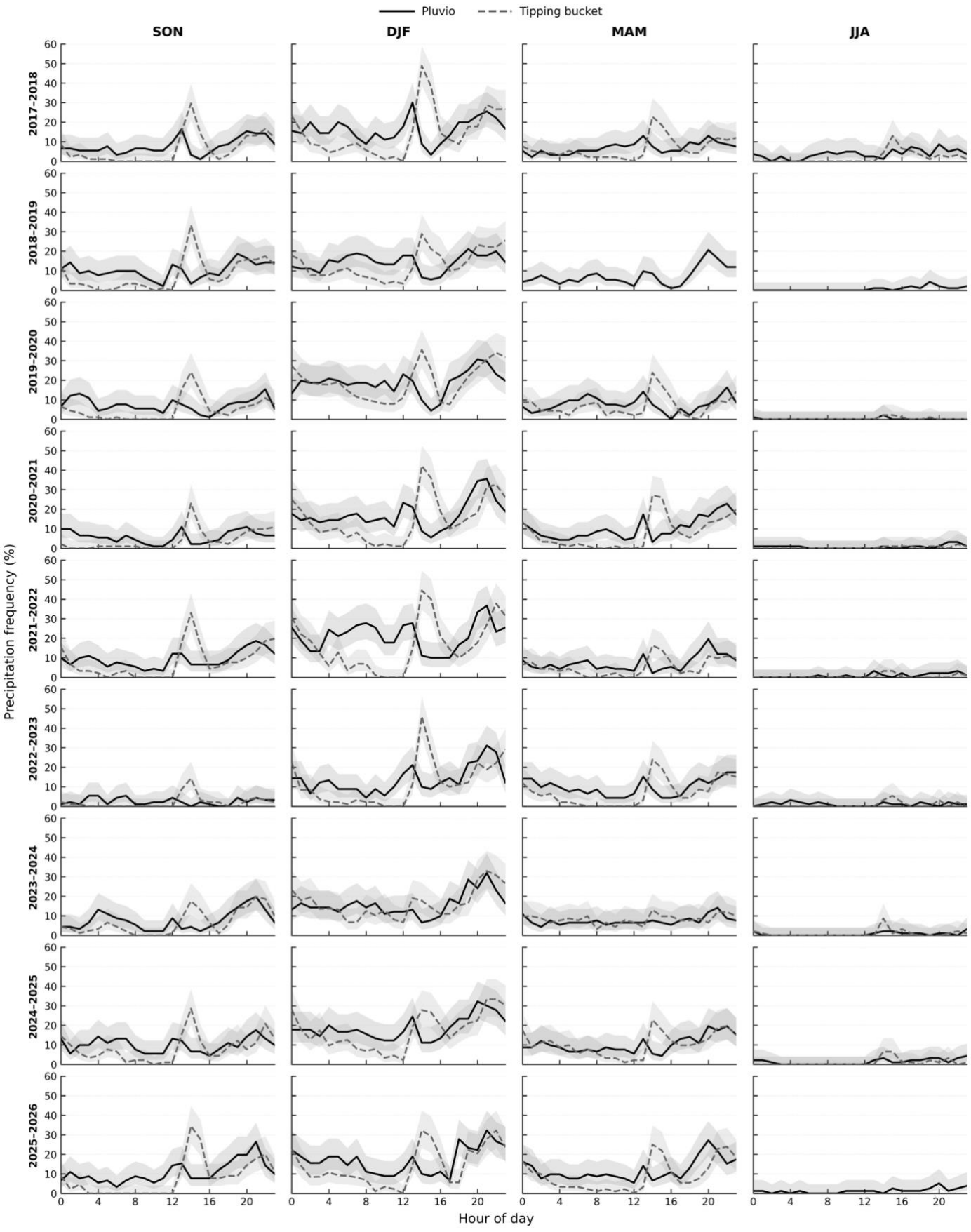


Figure S12. Seasonal diurnal cycles of precipitation frequency derived from tipping bucket and Pluvio² measurements at the Sibinacocha AWS across various hydrological years. Frequency computations were based on a threshold minimum precipitation rate of 0.1 mm hr⁻¹ and required at least 80% seasonal data completeness.

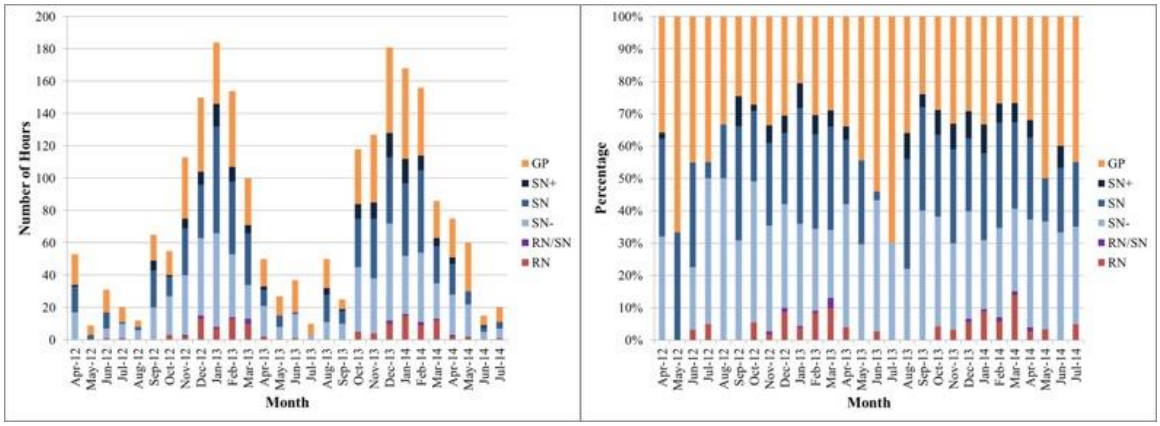


Figure S13. All precipitation hours at Murmurani from April 2012 to July 2014 by total number of hours (top) and total percentage (bottom) of each precipitation type by month. GP graupel; SN+ heavy snow; SN moderate snow; SN- light snow; RN/SN rain/snow mix; RN rain.